

Excited-State Density Distributions of Neutron-Rich Unstable Nuclei

J. Terasaki

School of Physics, Peking University, Beijing 100871, P. R. China

J. Engel

Department of Physics and Astronomy, University of North Carolina, Chapel Hill, NC 27599-3255

(Dated: August 7, 2018)

We calculate densities of excited states in the quasiparticle random-phase approximation (QRPA) with Skyrme interactions and volume pairing. We focus on low-energy peaks/bumps in the strength functions of a range of Ca, Ni, and Sn isotopes for $J^\pi = 0^+, 1^-,$ and 2^+ . We define an “emitted-neutron number”, which we then use to distinguish localized states from scattering-like states. The degree of delocalization either increases as the neutron-drip line is approached or stays high between the stability line and the drip line. In the 2^+ channel of Sn, however, the low-lying states, not even counting surface vibrations, are still fairly well localized on average, even at the neutron drip line.

PACS numbers: 21.10.Pc, 21.60.Jz

The structure of excited states in exotic nuclei has been much studied recently, both in nuclei between Li and O [1, 2, 3, 4] and in heavier Ca [5] and Sn [6] isotopes. Low-energy strength is often enhanced, and theorists have tried to understand the mechanisms responsible. Besides strength functions, they have examined transition densities, which can be measured and provide information on excited-state structure. Our earlier paper [7] contains an investigation of strength functions and transition densities in a large range of medium-heavy spherical nuclei, from one drip line to the other.

Transition densities tell us about where in the nucleus transitions occur; they reflect the spatial distribution of products of single-particle and single-hole wave functions and, as a consequence, are always localized, though they can be very extended near the neutron drip line. In nuclei near stability large transition strength implies collectivity, which in turn tends to cause localization (as we shall see in giant resonances). Near the drip line, however, the familiar connection between strength and collectivity is less systematic at low energies. Reference [7] shows many examples of behavior like that characterizing light halo nuclei and predicted for certain 0^+ states in heavy nuclei in Ref. [8]: large strength coming from non-collective transitions to very spatially-extended single-particle states. Those excited states are usually unbound, and may not even be quasibound, that is they may be completely delocalized scattering states [8].

In this letter we suggest a measure of localization and then investigate the extent to which the strong low-lying excited states are localized, independent of their collectivity. To uncover changes in structure near the drip line, we track the degree of localization as N increases in $J^\pi = 0^+, 1^-,$ and 2^+ channels. Localization, which we analyze by examining *diagonal* density distributions of the excited states, has not been systematically studied before and offers a new window into excitations in exotic neutron-rich nuclei.

We can adopt ideas from simple one-particle quantum mechanics to distinguish localized states from extended

ones. If the energy of a single particle in, e.g., a square-well potential is negative (Chap. 3 of Ref. [9]) then the tail of its wave function decays exponentially, and if the energy is positive the tail oscillates. In certain small positive-energy windows, however, the amplitude of the oscillating tail is much smaller than that of the wave function inside the potential. Such states are sometimes called “quasibound”, and the solutions that exhibit no enhancement inside are sometimes referred to as “scattering states.”

Of course we are dealing with many-body quantum mechanics and the asymptotic wave function depends on many coordinates. The tail of the one-body density, however, should still give us a measure of localization. In this letter, we use the Skyrme-QRPA wave functions (with the parameter set SkM* and volume pairing) from Ref. [7], in which we discussed transition densities, to obtain the diagonal density of excited-state k :

$$\begin{aligned} \rho_k^q(\mathbf{r}) &= \langle k | \sum_i^{N \text{ or } Z} \delta(\mathbf{r} - \mathbf{r}_i) | k \rangle \\ &= \sum_{KK'L;q} (-\psi_K^*(\mathbf{r})\psi_{K'}(\mathbf{r})u_K u_{K'} \\ &\quad + \psi_{\bar{K}}^*(\mathbf{r})\psi_{\bar{K}'}(\mathbf{r})v_K v_{K'}) \\ &\quad \times (X_{LK'}^k X_{KL}^k + Y_{KL}^k Y_{LK'}^k) + \rho_0^q(\mathbf{r}), \quad (1) \end{aligned}$$

where q is proton or neutron, \mathbf{r}_i is the position operator of particle i , $\psi_K(\mathbf{r})$ is a single-particle wave function in the canonical basis, and u_K and v_K are the associated occupation amplitudes. The QRPA amplitudes $X_{KK'}^k$ and $Y_{\bar{K}\bar{K}'}^k$ are assumed real, \bar{K} denotes the state conjugate to K , and we have used the convention $\psi_{\bar{K}}(\mathbf{r}) = -\psi_K(\mathbf{r})$. The summation is taken only for protons or neutrons, and in our numerical calculations we will use the Hartree-Fock (-Bogoliubov) approximation to the ground-state density $\rho_0^q(\mathbf{r})$. To obtain Eq. (1) we have used the excited-state

creation operator

$$O_k^\dagger = \frac{1}{2} \sum_{KK'} \left(X_{KK'}^k a_K^\dagger a_{K'}^\dagger - Y_{KK'}^k a_K a_{K'} \right), \quad (2)$$

$$X_{K'K}^k = -X_{KK'}^k, Y_{K'K}^k = -Y_{KK'}^k, \quad K < K', \quad (3)$$

where a_K^\dagger and a_K are the creation and annihilation operators for quasiparticles in the canonical state K .

If, as in all the calculations presented here, the ground state is spherically symmetric, the number of particles between two radii is just the integral over that well-defined region of $\rho_k^q(r)r^2$. We define the ‘‘emitted-neutron number’’ associated with the state k as

$$N_e(k) = 4\pi \int_{r \geq r_c} dr r^2 (\rho_k^n(r) - \rho_0^n(r)), \quad (4)$$

where r_c denotes the radius at which the density $\rho_k^n(r)$ begins to develop a scattering tail. If $N_e(k)$ is close to or larger than 1, then the excited state is scattering-like (not localized), and if $N_e(k)$ is appreciably smaller than 1, then the excited state qualifies as quasibound (localized). Intermediate cases are also possible, of course. If the pairing gap is not zero $\rho_k^n(r)$ does not integrate to the correct particle number¹; we therefore multiply $\rho_k^n(r)$ by a constant (at most a few percent from unity) to normalize it correctly.

Rather than focus on individual states, we want to examine peaks in the strength function, which can encompass several discrete states. We therefore define a strength-weighted average of the emitted-neutron number for the strongly excited states k within a given peak:

$$\bar{N}_e = \frac{1}{2} (\bar{N}_e^{\text{IS}} + \bar{N}_e^{\text{IV}}), \quad (5)$$

$$\bar{N}_e^{\text{IS}} = \frac{\sum_k S_k^{\text{IS}} N_e(k)}{\sum_k S_k^{\text{IS}}}, \quad \bar{N}_e^{\text{IV}} = \frac{\sum_k S_k^{\text{IV}} N_e(k)}{\sum_k S_k^{\text{IV}}}, \quad (6)$$

where S_k^{IS} and S_k^{IV} denote isoscalar and isovector transition strengths to the state k . The number of terms in the sums is between 1 and 10. We average the isoscalar and isovector quantities because both channels appear in low-energy strength-function peaks, particularly near the drip line. The giant resonances do not have this property, however, and for them we will use \bar{N}_e^{IS} or \bar{N}_e^{IV} as measures.

Before investigating the dependence of emitted-neutron number on N and Z , we need to see whether we can calculate it reliably. The tail of the nuclear density is

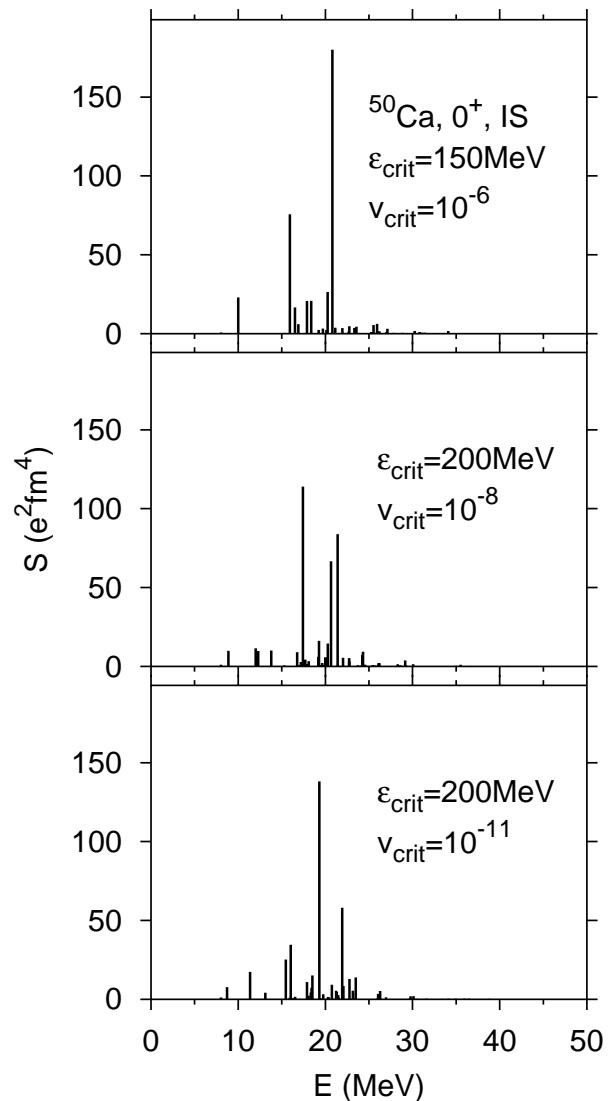


FIG. 1: Strength distributions in the isoscalar 0^+ channel of ^{50}Ca , with a box size 20 fm. The neutron chemical potential is -6.61 MeV.

extraordinarily sensitive, and converges slowly both with the size of our spatial ‘‘box’’ and the number of canonical states in our basis. Figure 1 shows the isoscalar 0^+ strength distribution for ^{50}Ca in a few versions of our calculation. We have varied two cutoff parameters: an upper limit ϵ_{crit} on canonical single-particle energies (for protons, which have a vanishing pairing gap), and a lower limit ν_{crit} on occupation amplitudes (for neutrons, which have a non-vanishing gap). We confirmed that when $\epsilon_{\text{crit}} = 250$ MeV and $\nu_{\text{crit}} = 10^{-14}$, the strength distribution is almost identical to that with $\epsilon_{\text{crit}} = 200$ MeV and $\nu_{\text{crit}} = 10^{-11}$, shown in the bottom panel. In Refs. [7, 10] we folded the strength to account for the 20-fm box radius, and the values $\epsilon_{\text{crit}} = 150$ MeV and $\nu_{\text{crit}} = 10^{-6}$ were sufficient for convergence of the strength function and transition densities to the level of accuracy we required. Figure 1 seems to suggest, however, that larger

¹ The QRPA does not guarantee the conservation of a quantity that is of second order or higher in the X ’s and Y ’s.

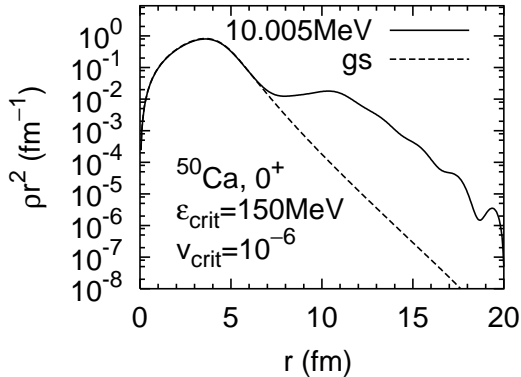


FIG. 2: Neutron-density distribution of the low-energy state with non-negligible strength in ^{50}Ca (see Fig. 1), calculated with $\varepsilon_{\text{crit}} = 150$ MeV, $v_{\text{crit}} = 10^{-6}$, and a box radius of 20 fm. The excitation energy is at the top of the figure. The ground-state density distribution (gs) is also drawn. In this case, $r_c = 7$ fm.

spaces are required to reproduce the tiny part of the excited-state density that lies significantly outside the nucleus.

To examine the issue more closely, we show in Fig. 2 the neutron density distribution associated with a low-lying state in the top part of Fig. 1; that distribution was obtained with the cutoff parameters we used extensively in Ref. [7]. In Fig. 3 we show the neutron densities associated with the corresponding states in the bottom part of Fig. 1, obtained in a larger space. The tails of the more accurate densities are noticeably different (and more realistic). Yet improving the description this way has a relatively small effect on the emitted-neutron number. In the smaller space the \bar{N}_e of low-energy states is 0.84, with individual $N_e(k)$ ranging from 0.77 to 0.90, and in the larger space it is 0.89, with $N_e(k)$ ranging from 0.85 to 0.92. These ranges, 10% or less of the average, are not only small, but also typical of cases with \bar{N}_e near 1. Changing the box radius to 25 fm fragments the strength by adding new states, so that the $N_e(k)$ cannot really be tracked as the box size changes. The average \bar{N}_e over the states in a certain energy range, however, turns out to be a fairly robust measure of localization; with a box size of 25 fm, $\bar{N}_e = 0.86$ for 5 sample states. Perhaps the stability of \bar{N}_e , an integrated quantity, is not so surprising given that the smaller space is large enough to describe the wave functions extremely well for r less than r_c . In any event, we can conclude here — for the 0^+ bump below the giant resonance in ^{50}Ca — that the states are scattering-like. Nearly a full neutron is far outside the nucleus, no matter how we vary parameters.

To set a benchmark of sorts, we have looked at densities for giant resonances in the isoscalar and isovector 0^+ , 1^- , and 2^+ channels of several Ca, Ni, and Sn isotopes near stability. \bar{N}_e^{IS} and \bar{N}_e^{IV} are always on the order of 0.5 or less. The isoscalar giant dipole resonances have

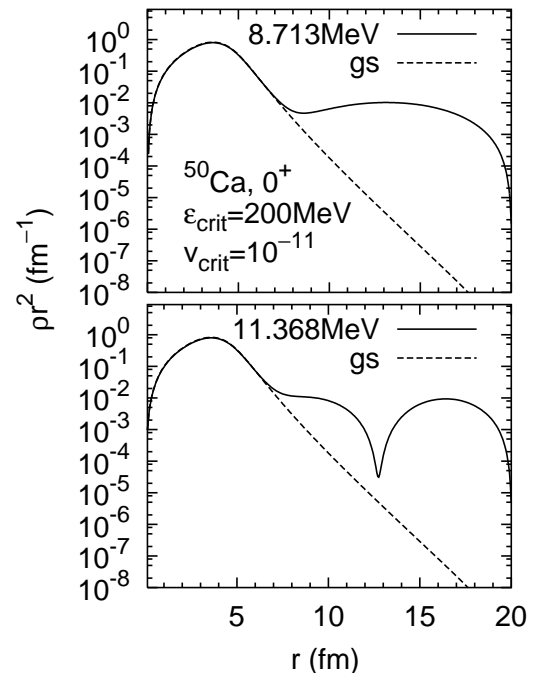


FIG. 3: The same as Fig. 2 but for $\varepsilon_{\text{crit}} = 200$ MeV and $v_{\text{crit}} = 10^{-11}$.

the largest values. The smallest belongs to the isovector giant quadrupole resonance of ^{58}Ni , with $\bar{N}_e^{\text{IS}} = 0.01$. The reasons for this very small value are that the main components of the neutron excitation involve deep hole states and particle states near the Fermi surface, and that protons contribute appreciably.

Having established a good measure of localization and calibrated it for typical collective resonances, we are now in a position to examine the behavior of low-lying excitations in neutron-rich nuclei. In each channel we look at low-energy bumps in a range of Ca, Ni, and Sn isotopes. The resulting \bar{N}_e , plotted versus N , appear in Fig. 4. For 0^+ states they are more or less constant, at least in Ca and Sn, and since the constant is greater than 0.8, the wave functions in the bumps are not localized. The \bar{N}_e in the 1^- channel in Ca and Ni show a clear increase with N , from 0.1 to about 1; those states are localized near stability and become more scattering-like towards the drip line. The 1^- states in Sn are harder to interpret; the curve has a maximum of about 0.8 around $N = 100$, but shows no clear trend in one direction or the other. The 2^+ states in Ca and Ni mirror the behavior of the 1^- states. In the 2^+ channel of Sn, \bar{N}_e increases with N but the low-lying states never get less localized than typical giant resonances. By our criterion, those states are localized, on average, even at the drip line, though they fluctuate within a given peak in a way that cannot be seen in the average (some individual states have $N_e(k) > 0.8$). We should note that the states used to determine \bar{N}_e do *not* include low-lying surface quadrupole

vibrations, which usually have $N_e(k) < 0.1$.

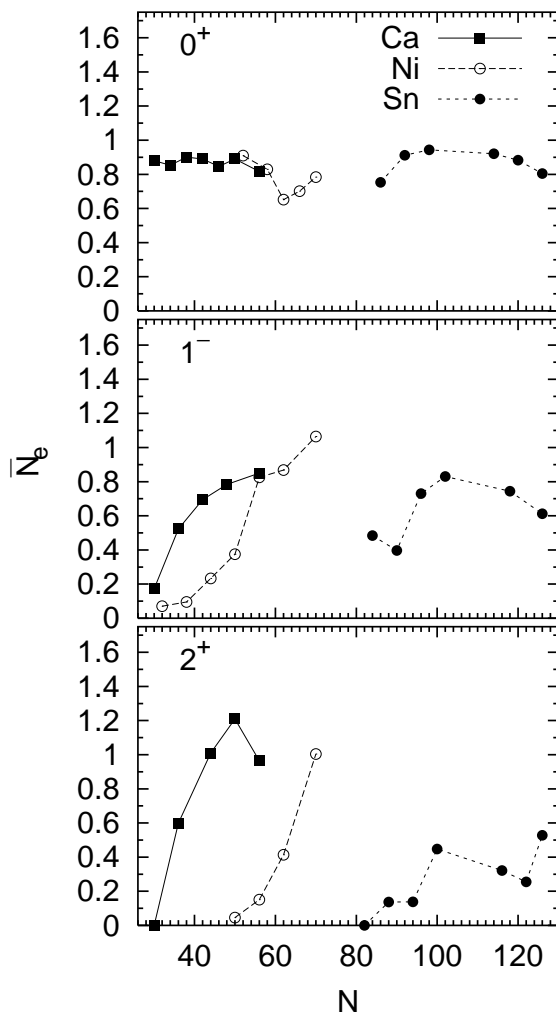


FIG. 4: \bar{N}_e in low-lying strength-function peaks, versus N , for the 0^+ , 1^- , and 2^+ channels of a sequence of Ca, Ni, and Sn isotopes. In the 2^+ channel, the lowest-energy states (surface vibrations), carrying the largest strengths, are not included. In Ni the 1^- curve has more points than those of the other J^π channels because the low-energy bump first appears at smaller N .

In Ref. [7] we found that the strength to low-lying bumps grew with N in essentially every channel and every isotopic chain. Though we sometimes see similar behavior in N_e , it is not universal. The 0^+ states, for instance, are not localized even near stability. And the 2^+ states in Sn, while they become more scattering-like with increasing N , do not always delocalize beyond the level of giant resonances. All this comes with a caveat, however: it is possible that many-particle many-hole states that admix with QRPA excitations can alter \bar{N}_e somewhat. The one-particle one-hole nature of our states means, for instance, that \bar{N}_e is never much greater than one. Calculating the structure of many-particle many-hole states is difficult, however, and it may be some time before a systematic study of the kind reported here can be made.

To summarize quickly: giant resonances consistently have \bar{N}_e around 0.5. In low-energy peaks \bar{N}_e is more varied, and changes with neutron number in ways that depend both on the isotopic chain and on multipolarity. Strongly excited low-energy states near the drip line are sometimes scattering states, but not always.

This work was funded in part by the U.S. Department of Energy under grant DE-FG02-97ER41019. We thank W. Nazarewicz for useful discussion and the National Center for Computational Sciences at Oak Ridge National Laboratory and Information Technology Services at University of North Carolina at Chapel Hill for the use of their computers. Parts of this research were done when one of us (J.T.) was at the University of North Carolina and at RIKEN.

-
- [1] M. Zinser, F. Humbert, and T. Nilsson et al., Nucl. Phys. **A619**, 151 (1997).
 [2] R. Palit, P. Adrich et al., Phys. Rev. C **68**, 034318 (2003).
 [3] T. Nakamura, N. Fukuda, and T. Kobayashi et al., Phys. Rev. Lett. **83**, 1112 (1999).
 [4] E. Tryggestad, T. Baumann, and P. Heckman et al., Phys. Rev. C **67**, 064309 (2003).
 [5] T. Hartmann, M. Babilon, and S. Kamerdzhiev et al., Phys. Rev. Lett. **93**, 192501 (2004).
 [6] P. Adrich, A. Klimkiewicz, and M. Fallot et al., Phys. Rev. Lett. **95**, 132501 (2005).
 [7] J. Terasaki and J. Engel, nucl-th/0603062, submitted to Phys. Rev. C (2006).
 [8] I. Hamamoto, H. Sagawa, and X.Z. Zhang, Phys. Rev. C **53**, 765 (1996).
 [9] A. Messiah, *Quantum Mechanics* (North Holland, Amsterdam, 1961).
 [10] J. Terasaki, J. Engel, and M. Bender et al., Phys. Rev. C **71**, 034310 (2005).